Journal of
Water & Climate Change

Journal of Water and Climate Change Vol 15 No 4, 1532 doi: 10.2166/wcc.2024.409

Long-term dynamics of remote sensing indicators to monitor the dynamism of ecosystems in arid and semi-arid areas: contributions to sustainable resource management

Hadjer Keria [a,*], Ettayib Bensaci [b], Asma Zoubiri [b] and Zineb Ben Si Said [a]

[a] Laboratory of Biodiversity and Biotechnological Techniques for the Valorisation of Plant Resources (BBT_VPR), Department of Natural and Life Sciences, University of Mohamed Boudiaf, M'sila 28000, Algeria
[b] Department of Natural and Life Sciences, University of Mohamed Boudiaf, M'sila 28000, Algeria
*Corresponding author. E-mail: hadjer.keria@univ-msila.dz

HK, 0000-0002-7539-0571

ABSTRACT

Climate change's impact on wetlands has heightened concerns regarding the growing incidence of drought. It is imperative to continuously monitor long-term changes in wetlands to detect variations. This study evaluates the enduring variability of remote sensing indicators within 25 watershed areas in Algeria, recognized for their substantial biodiversity. We employed two robust statistical techniques (linear regression and the Mann-Kendall test) with data from diverse sources, including MODIS satellite data. From a time-series dataset spanning 22 years, we assembled several pivotal indicators: normalized difference vegetation index (NDVI), enhanced vegetation index (EVI), normalized difference water index (NDWI), and land surface temperature (LST), selected to evaluate vegetation and water stress within the study areas. Our analysis revealed that NDVI showed more conspicuous temporal response when compared with EVI and NDWI. We uncovered negative correlations between NDVI and LST, underscoring the influence of drought and plant stress on vegetation within the study areas ($R^2 = 0.109$ to $R^2 = 0.5701$). Our Mann-Kendall trend analysis underscored the significance of NDVI and its robust association with EVI and NDWI. Understanding the dynamics of vegetation and water stress is of paramount importance for projecting changes in ecosystems, particularly within water bodies subject to climate variability.

Key words: Algeria, indicators, remote sensing, vegetation, watersheds

HIGHLIGHTS

- Study reveals increasing drought events in water bodies due to climate change.
- Assessing remote sensing indicators in 25 biodiverse watersheds aids biodiversity conservation efforts.
- The research underscores the crucial role of remote sensing technology in identifying fluctuations and aiding biodiversity conservation.
- Understanding vegetation and water stress dynamics is vital for accurate ecosystem forecasts.

GRAPHICAL ABSTRACT

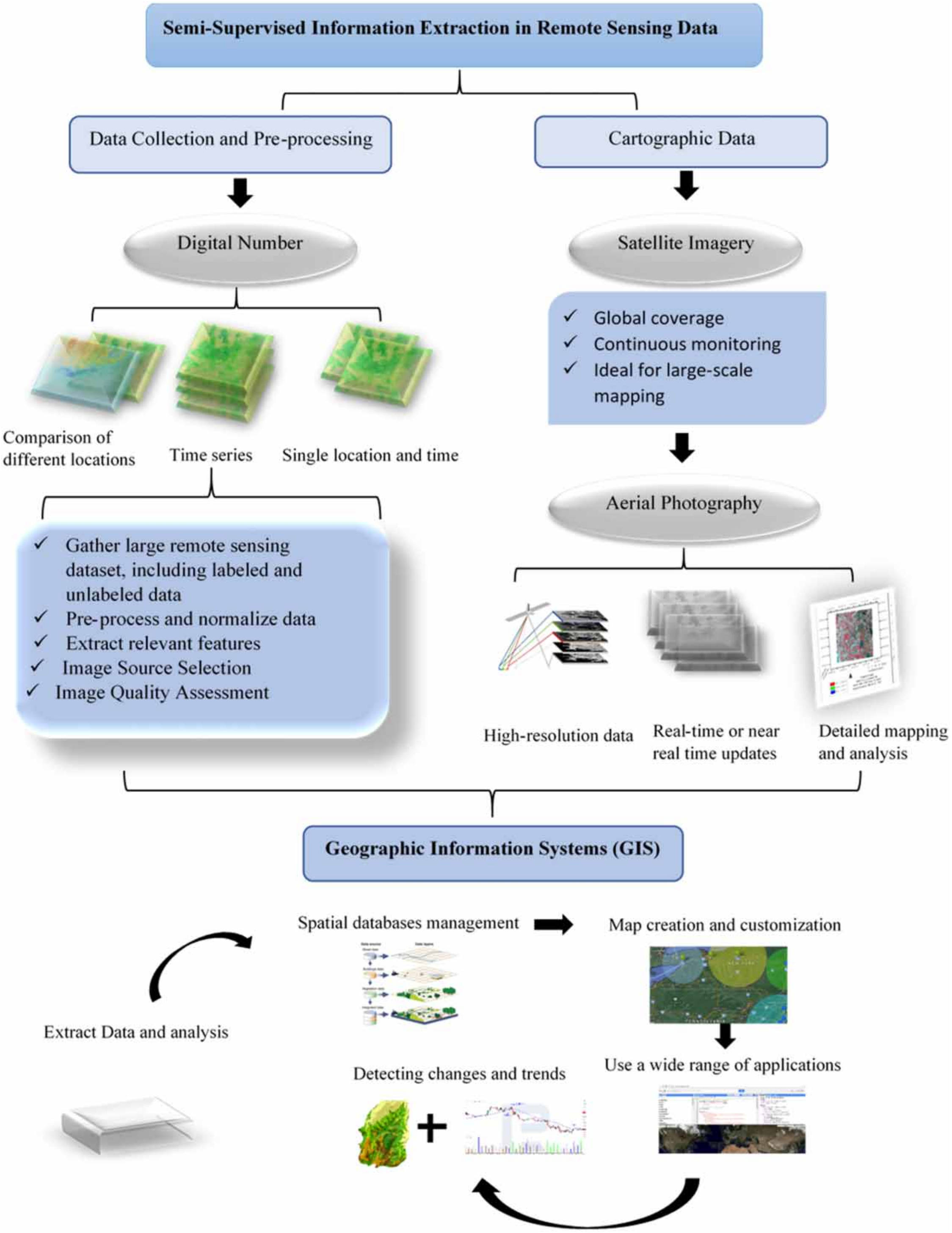

1. INTRODUCTION

The Earth's ecosystem has undergone rapid and extensive transformations over the past five decades, representing unprecedented changes not previously observed. Vegetation plays a foundational role within this ecosystem, and alterations in vegetation have far-reaching implications for global climate dynamics and the carbon cycle. A substantial body of evidence supports the assertion that nearly all terrestrial ecosystems are experiencing degradation, largely attributed to human activities and the pervasive impacts of global warming (Stellmes *et al.* 2010; Yang *et al.* 2017).

Remote sensing has significantly transformed our perception, utilization, and management of land assets (Huang *et al.* 2020). Numerous Earth observation programs have facilitated the generation of increasingly comprehensive insights into the wide array of natural variations and anthropogenic activities taking place on the Earth's surface. This is achieved through spectral analysis of the environment, enabling us to decipher valuable information from the data. The recording of data in time series has played a pivotal role in disseminating this knowledge (Potter *et al.* 2003).

Remotely sensed multi-spectral imagery contains bands to create a composite image that can be viewed and analyzed (Xue & Su 2017). Advancements in robust and widely accessible remote sensing imagery enable the development of new methodologies for evaluating assessments at broad, medium, and fine scales. This allows for the detection of persistent structural and functional environmental transformations (Nagendra *et al.* 2013; O'Connor *et al.* 2015). A variety of tools and methodologies have been developed and rigorously assessed to gauge the condition of natural resources, encompassing their responses to climate change (CC), extreme events, and human-induced stresses. Among these methods, geospatial techniques, notably remote sensing (RS), have been instrumental. Groundwater sustainability tools (GSTs) have been extensively employed in diverse research initiatives, providing insights into various aspects of water resources. For instance, Moumane *et al.* (2021) utilized GSTs to assess the state of groundwater resources. This approach enables a comprehensive evaluation of the health and sustainability of groundwater reservoirs. In other studies, the integration of geographic information system (GIS) and RS techniques, as demonstrated by Ben Salem *et al.* (2019) and Ougougdal *et al.* (2020), facilitated the examination of water erosion.

From a scientific perspective, there exists a diverse array of methodologies available for investigating the repercussions of CC on drought events. Among these, the normalized difference vegetation index (NDVI) stands as a commonly utilized tool for assessing the impacts of both drought and CC. One notable study conducted by Nanzad *et al.* (2019) effectively harnessed the NDVI anomaly as a tool for assessing drought conditions and investigating their relationship with various climatic factors over the period spanning from 2000 to 2016. In a related endeavor, Xie & Fan (2021) developed drought indicators by leveraging vegetation indices, specifically the NDVI and enhanced vegetation index (EVI). These indices were derived from data acquired through the Moderate Resolution Imaging Spectroradiometer (MODIS), offering a comprehensive view of vegetation changes in response to drought. Furthermore, the normalized difference water index (NDWI) has emerged as a significant tool for the analysis of hydrological droughts, as elucidated by Noorisameleh *et al.* (2020). This index aids in assessing variations in water content and availability, which are crucial aspects of hydrological drought events.

The indices, including the NDVI, NDWI, and EVI, are widely employed for surface observations. Their utility in evaluating the impacts of CC on drought conditions underscores their importance in advancing our understanding of these complex environmental phenomena.

The NDVI is a credible indicator of broad-scale transformations in vegetation density (Myneni *et al.* 1995; Wang *et al.* 2018). It has been extensively used for monitoring the vegetation dynamics in surveillance and estimating the vegetation feedback on a global scale (Nemani *et al.* 2003; Zhu *et al.* 2016) and regional scales (Piao *et al.* 2003; Wu *et al.* 2015). Over the last few decades, the global climate has witnessed some dramatic shifts. Furthermore, global warming has been shown to be undeniable (Karl & Trenberth 2003; IPCC 2023). Accordingly, in recent decades, there has been an increasing emphasis on the significant modifications observed in the Earth's climate and their implications for greening development (De Jong *et al.* 2011; Kong *et al.* 2020; Guo *et al.* 2021).

In the last several years, Algeria has suffered from the deterioration of its wetlands (Nedkov *et al.* 2018), confirming the results of previous studies (Sitayeb & Benabdeli 2008; Belgherbi & Benabdeli 2010; Ghodbani & Amokrane 2013; Megharbi *et al.* 2016; Souidi *et al.* 2016; Keria *et al.* 2023). Algeria comprises 1,451 wetlands, consisting of 762 natural areas and 689 artificial areas (some of which are included in the list of globally significant wetlands) (DGF 2017). In 2009, 42 Ramsar sites were classified, from the international agreement adopted in 1971 that deals with wetlands of international importance, as essential habitats for the Convention on Biological Diversity. This treaty recognizes the ecological, economic, and cultural importance of wetlands, thereby encouraging the preservation and sustainable use of these diverse ecosystems (Ramsar 2015), spanning a combined area of 2.960 million hectares. Among these conserved sites, saline lakes account for 45.23% of the coverage, estimated at roughly 2.07890 million hectares (Koopmanschap *et al.* 2011). These wetlands are typically found in coastal areas or valleys conducive to socio-economic growth, making them susceptible to being targeted for urban, agricultural, or industrial development. Their worldwide surface area has diminished by 64% and 71%, respectively, since 1900 (Davidson 2014). It should be noted that the weakness or lack of a management system for watersheds in Algeria significantly affects decisions and professionals involved in the management of wetland environments.

As the existing body of study in this particular field demonstrates a dearth of current investigations that employ rigorous statistical (remote sensing) approaches in a susceptible region affected by CC and anthropogenic activities. In light of this deficiency, in this study, the main focus is on understanding the spatial and temporal changes in 25 wetland areas located in Algeria, given their environmental and economic significance. Among the specific objectives of the study are the following: (1) to examine the temporal pattern of EVI, NDVI, NDWI, and LST indicators in a variety of water catchments in Algeria during the period from 2000 to 2022; (2) assessment of the influence of CCs on Algeria's watersheds using Google Earth Engine (GEE) data; (3) identification of environmentally sensitive areas in Algeria's watersheds.

2. MATERIALS AND METHODS

2.1. Study area

Algeria is located in North Africa and spans an area of 2,381,741 km^2. It stretches along the Mediterranean Sea from east to west for approximately 1,200 km and extends from north to south for nearly 2,000 km. The northern part of Algeria encounters a Mediterranean climate distinguished by sweltering summers, mild winters, and significant rainfall. In contrast, the southern region exhibits a climate with hot summers, cold winters, and limited precipitation, particularly in the high plains south of the Atlas Mountains. Due to the Sahara Desert covering approximately 80% of the country, Algeria experiences extremely high temperatures in the summer. Winter temperatures can drop below 0°C in some regions, with daytime temperatures typically being moderate and night-time temperatures being low. The area of study encompasses a variety of slopes with distinct hydrological characteristics, specific current statuses, and climate diversity in Algeria's wetland complex, as described in Table 1. Notable sites among the permanent watercourses include Macta Marsh, Great Sebkha, Telamine Lake, Arzew saline, Boughezoul dam, Chott Zehrez Chergui, Chot Ech Chergue, Dayet El Ferd, Chutt Zehres Gharbi, and Chott El Hodna. These regions, all classified as semi-arid, enjoy a Ramsar designation that underscores their ecological importance. However, irregular hydrological variations characterize areas such as Chott Melghir, Beni Bahdel dam, Bougara dam, Bouhanifia dam, Chorfa dam, Cheliff dam, Dahmoni dam, Gargar dam, Karrada dam, Ksob dam, and Sarno dam. Despite being semi-arid, these sloping basins pose particular water management challenges. Additionally, the study area includes arid environments, such as Chott Merouane and Chott Ain El Beida, which are characterized by irregular hydrology. Chott Merouane is also identified as an Important Bird and Biodiversity Area (IBA) with a Ramsar designation. These arid areas contribute a unique dimension to the hydrological complexity of the region. Finally, permanent sites, such as El Golea Ramsar (2004) in an arid area and Chott Ain El Beida Ramsar (2004) in a semi-arid context, complement the environmental mosaic of the study area (Figure 1). Wetland areas selected for study in Algeria were chosen based on their environmental and economic significance, particularly given their classification by Ramsar, an international organization dedicated to the conservation and sustainable use of wetlands.

2.2. Data and processing

The data analyzed in this research were collected from the GEE platform (https://developers.google.com/earth-engine/datasets/). The platform hosts a vast array of remote sensing datasets and is equipped with robust data processing capabilities (Gorelick *et al.* 2017). In this study, we utilized a dataset that includes MODIS. The research period for this work spans from 2000 to 2022.

The MOD11A1, MOD09GA, and MOD13Q1 products were utilized in our study, as these datasets provide essential information for variables such as the NDVI, EVI, NDWI, and land surface temperature (LST). The sources and characteristics of the various datasets utilized in this work are listed in Table 2.

2.3. Method

2.3.1. Assessment of NDVI temporal dynamics

The NDVI is utilized to quantify the variability of visible and near-infrared light in vegetation. This is achieved by calculating the difference between these spectral bands within specific wavelength ranges and normalizing it across the entire spectrum. The NDVI is calculated using the equation (NIR−VIS)/(NIR + VIS), where NIR represents the spectral reflectance in the near-infrared band and VIS represents the reflectance in the visible band. These indicators have been extensively employed

Table 1 | Characteristics of all the study areas

Watershed	Watershed area (ha)	Water quality	Hydrological cadency	Current status	Latitude (N)	Longitude (E), (W)	Climate
Macta Marsh	44,500	Salty	Permanent	Ramsar (2001)	35.704670°	-0.121092°W	Semi-arid
Great Sebkha	56,870	Salty	Permanent	Ramsar (2001)	35.518985°	-0.860435°W	Semi-arid
Telamine Lake	2,399	Salty	Permanent	Ramsar (2004)	35.736568°	-0.382841°W	Semi-arid
Arzew saline	5,778	Salty	Permanent	Ramsar (2004)	35.860485°	-0.329562°W	Semi-arid
Boughezoul dam	9,058	Salty	Permanent	Ramsar (2011)	35.738283°	2.785820°E	Semi-arid
Chott Zehrez Chergui	50,985	Salty	Permanent	Ramsar (2003)	34.944018°	2.862758°E	Semi-arid
Chott Ech Chergui	855,500	Salty	Permanent	Ramsar (2001)	34.350000°	0.500000°E	Semi-arid
Dayet El Ferd	3,323	Salty	Permanent	Ramsar (2004)	34.497783°	-1.245122°W	Semi-arid
Chott Zehrez Gharbi	52,200	Salty	Permanent	Ramsar (2003)	34.944018°	2.862758°E	Semi-arid
Chott El Hodna	362,000	Salty	Permanent	Ramsar (2001)	35.442812°	4.797680°E	Semi-arid
Chott Melghir	551,500	Salty	Irregular	Ramsar (2002)	34.122969°	6.001930°E	Arid
Beni Bahdel dam	54,630	Salty	Irregular	Not protected	34.703221°	-1.500366°W	Semi-arid
Bougara dam	11,320	Salty	Irregular	Not protected	35.565565°	1.908756°E	Semi-arid
Boughrara dam	175,450	Salty	Irregular	Not protected	34.874073°	-1.653459°W	Semi-arid
Bouhanifia dam	34,520	Salty	Irregular	Not protected	35.278106 °	-0.071455°W	Semi-arid
Chorfa dam	70,210	Salty	Irregular	Not protected	35.384663°	-0.274070°W	Semi-arid
Cheliff dam	50,000	Salty	Irregular	Not protected	35.990491°	0.446296°E	Semi-arid
Chott Merouane	337,700	Salty	Irregular	IBA-Ramsar (2001)	33.5328°	6.1034°E	Arid
Dahmoni dam	39,520	Salty	Irregular	Not protected	35.451481°	1.449635°E	Semi-arid
Gargar dam	358,280	Salty	Irregular	Not protected	35.913654°	1.007704°E	Semi-arid
Karrada dam	65,000	Salty	Irregular	Not protected	36.058190°	0.384113°E	Semi-arid
Ksob dam	22,720	Salty	Irregular	Not protected	35.838615°	4.565161°E	Arid
Sarno dam	21,250	Salty	Irregular	Not protected	35.294987°	-0.594364°W	Semi-arid
El Golea	18,947	Salty	Permanent	Ramsar (2004)	30.625869°	2.875530°E	Arid
Chott Ain El Beida	6,853	Salty	Irregular	Ramsar (2004)	31.800687°	5.494661°E	Arid

to capture the dynamics and growth of vegetation (Tucker *et al.* 1986; Myneni *et al.* 1997; Nemani *et al.* 2003; Piao *et al.* 2011; Donohue *et al.* 2016).

The trends of NDVI for each pixel were analyzed using linear regression from 2000 to 2022. The equation formula used for the linear analysis is as follows (Hu *et al.* 2019):

$$\text{Slope} = \frac{n \times \sum_{i=1}^{n} i \times \text{NDVI}_I - \sum_{i=1}^{n} i \sum_{i=1}^{n} \text{NDVI}_i}{n \times \sum_{i=1}^{n} i^2 - \left(\sum_{i=1}^{n} i\right)^2}$$

In the provided equation, 'Slope' represents the change in NDVI (NDVI_i) over time; NDVI_i is the NDVI value calculated using the formula for the i-th year; and n represents the total number of years during the assessment duration. The 'Slope' indicates the rate of change in vegetation growth. If the Slope > 0, it suggests an increase in vegetation development with a decrease in vegetation coverage. When the Slope $= 0$, it indicates stable and consistent regional vegetation growth. On the other hand, if the Slope < 0, it suggests a decrease in vegetation development activity with an increase in vegetation coverage (Zhe & Zhang 2021).

2.3.2. Determination of different remote sensing indices

The NDWI was utilized in this study to evaluate the hydrological condition of the wetlands. This index was specifically designed to enhance the visibility and discrimination of open water features in remotely sensed imagery. The NDWI

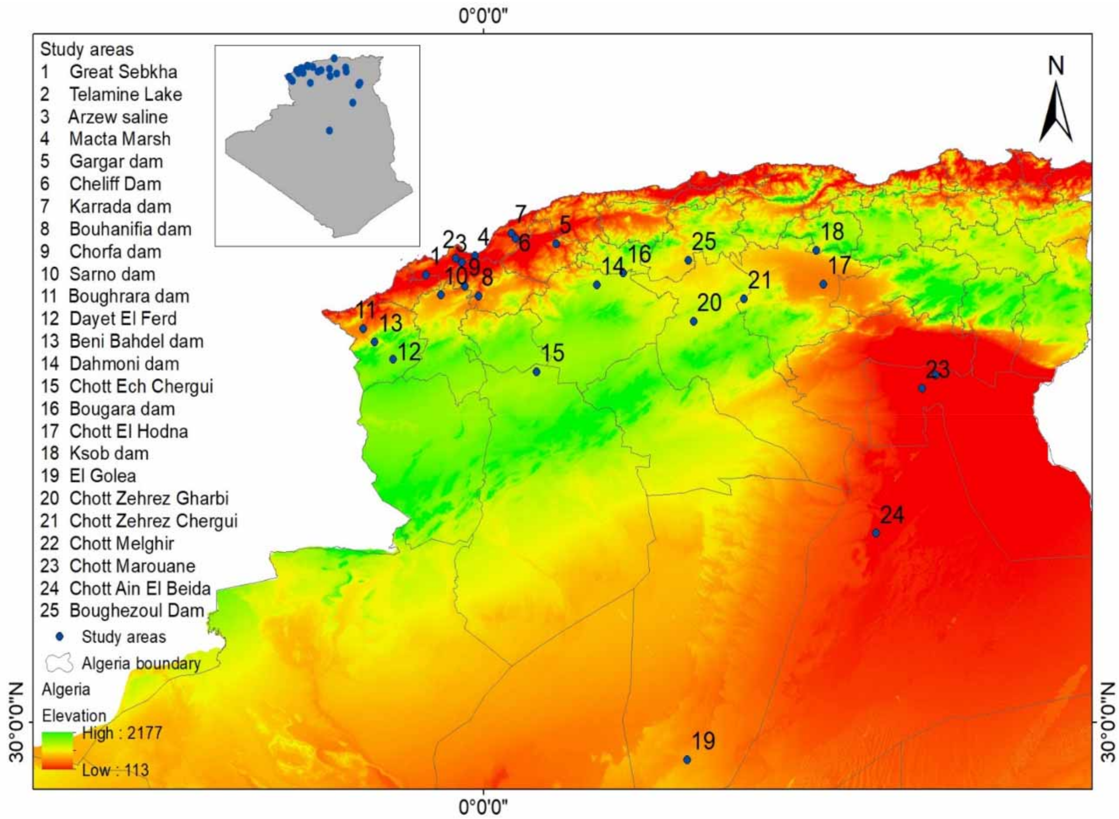

Figure 1 | Locations of all the study areas in Algeria.

Table 2 | Datasets utilized in this study

Data products	Data types	Spatial resolution	Temporal resolution	Spatial coverage	Duration
MOD09GA	NDWI	250 m	16 days	Global	2000–2022
MOD13Q1	NDVI/EVI	250 m	16 days	Global	2000–2022
MOD11A1	LST	1,000 m	8 days	Global	2000–2022

values vary between −1 and 1. In principle, NDWI values greater than zero indicate the presence of water bodies, while values less than zero indicate non-water areas. The calculation of NDWI is performed as follows (McFeeters 1996):

$$\mathrm{NDWI} = \frac{\mathrm{NIR} - \mathrm{RED}}{\mathrm{NIR} + \mathrm{RED}}$$

The spatial resolution of MODIS LST products is low, which limits their accuracy for environmental analysis and tracking rapid changes in land use (Chen *et al.* 2006). However, if the relationships between land use and long-term changes are not affected by the low spatial resolution, they can still be utilized to estimate high-precision changes in land use over time. To address this limitation, a method has been developed to enhance the spatial resolution of rapid metrics by using a high-precision spatial spectrometer. The underlying concept is that the quantitative relationship between the spectral index remains consistent under various circumstances, allowing the relationship derived from low-spatial-resolution spectrometers to be applied to high-spatial-resolution LST products. The calculation formula is as follows (Wang *et al.* 2014; Hua *et al.* 2018):

$$T_h = f(\mathrm{SI}_h) + \Delta T_C$$

$$\Delta T_C = T_c - f(\mathrm{SI}_C)$$

Here, SI_C and SI_h are low- and high-resolution spectral indexes, respectively; T_c and T_h indicate LST at low and high resolutions, respectively (Xu *et al.* 2021).

The EVI compensates for some climatic variations and background noise related to vegetation and is more sensitive in areas with dense vegetation. The calculation of the indicator includes the value of L to offset the background of the canopy, the values of C as atmospheric resistant factors, as well as values from the blue range. In most cases, this improvement allows the calculation of the indicator as a ratio between R (red) and NIR (near-infrared) values while minimizing background noise, ambient noise, and saturation. C_1 and C_2 are aerosol-proof factors that use the blue range to correct aerosol effects in the red range. Additionally, ρ represents the reflection of the air- or partially atmospheric-adjusted surface, while L addresses the background modulation of the canopy, dealing with the transport of non-linear radiation and spectral differences between NIR and R through the canopy. Some of the algorithmic parameters used in EVI are $L = 1$, $C_1 = 6$, $C_2 = 7.5$, and G (gain or profit factor) $= 2.5$. The formula is presented as follows (Huete *et al.* 1994, 1997):

$$\mathrm{EVI} = G\frac{\rho_{\mathrm{NIR}} - \rho_{\mathrm{RED}}}{\rho_{\mathrm{NIR}} + C_1 \times \rho_{\mathrm{RED}} - C_2 \times \rho_{\mathrm{BLUE}} + L}.$$

2.3.3. Mann–Kendall trend analysis

The Mann–Kendall (MK) test is applied to evaluate if a variable trend over time is monotonic upward (growing) or downward (reducing) (Mann 1945; Kendall 1975). The test calculates the slope using Sen's slope estimator (Sen 1968), which is a non-parametric rank-based method used to detect significant trends in time-series data (Tabari *et al.* 2011; Suryavanshi *et al.* 2014; Gajbhiye *et al.* 2016; Pingale *et al.* 2016; Kumar *et al.* 2017). The MK statistics are computed as follows:

$$S = \sum_{i=1}^{n-1}\sum_{j=i+1}^{n} \mathrm{sgn}(y_j - y_i)$$

When the comparison $(y_j - y_i)$ is positive, the value is 1, when it is negative, the value is -1, and when it is 0, the value is 0. This S number represents the time-series' trend; if S is positive, the trend is rising; if S is negative, the trend is falling. The S value is necessary for evaluating the MK value, which is as follows:

$$t = S/(n(n-1)/2).$$

3. RESULTS

3.1. The evolving pattern of NDVI in the 25 areas over the course of the last 22 years

The linear trend analysis of NDVI from 2000 to 2022 in various regions of Algeria reveals significant patterns. The average yearly NDVI values in the study areas ranged from 0 to 0.7, with an overall average between 0.098% and 0.34% (Figure 2). The analysis indicates a gradual decrease in NDVI values from the northwest coast towards the eastern and western interior areas and further to the southern regions of Algeria. This suggests that environmental conditions are generally more favorable in the northwest regions compared with the interior and southern regions.

Specifically, elevated NDVI values, ranging between 0.4 and 0.6, were observed in certain areas, while lower values, predominantly ranging from 0 to 0.2, were more prevalent. The Sarno watershed stood out with the highest NDVI value in 2001, exceeding 0.6, while the Chott Merouane watershed recorded the lowest NDVI value of 0.07 in 2006.

In the upper reaches of the region, the 22-year average NDVI was 0.4, indicating a moderate overall vegetation level. There was an upward trend in vegetation from inland areas towards the northwest. Among specific areas, the Chott Merouane area in the northeast of the North Sahara had the lowest vegetation proportion, followed by the Golea Basin, Chott Melrhir, Ain Beida, Chott El Hodna, and Ksob dam. In contrast, the highest vegetation ratios were observed in areas such as the Sarno dam, Telamine Lake, Arzew Saline, Macta Marshes, Great Sebkha, Boughrara dam, Cheliff dam, Chorfa dam, Beni Bahdel dam, Karrada dam, and Bouhanifia dam, located in the northwest. Bougara dam, Dahmoni dam, and Gargar dam, situated in the central and upper reaches of the region, also had relatively high vegetation cover, with an annual average NDVI for these areas reaching 0.6, indicating medium to high vegetation levels.

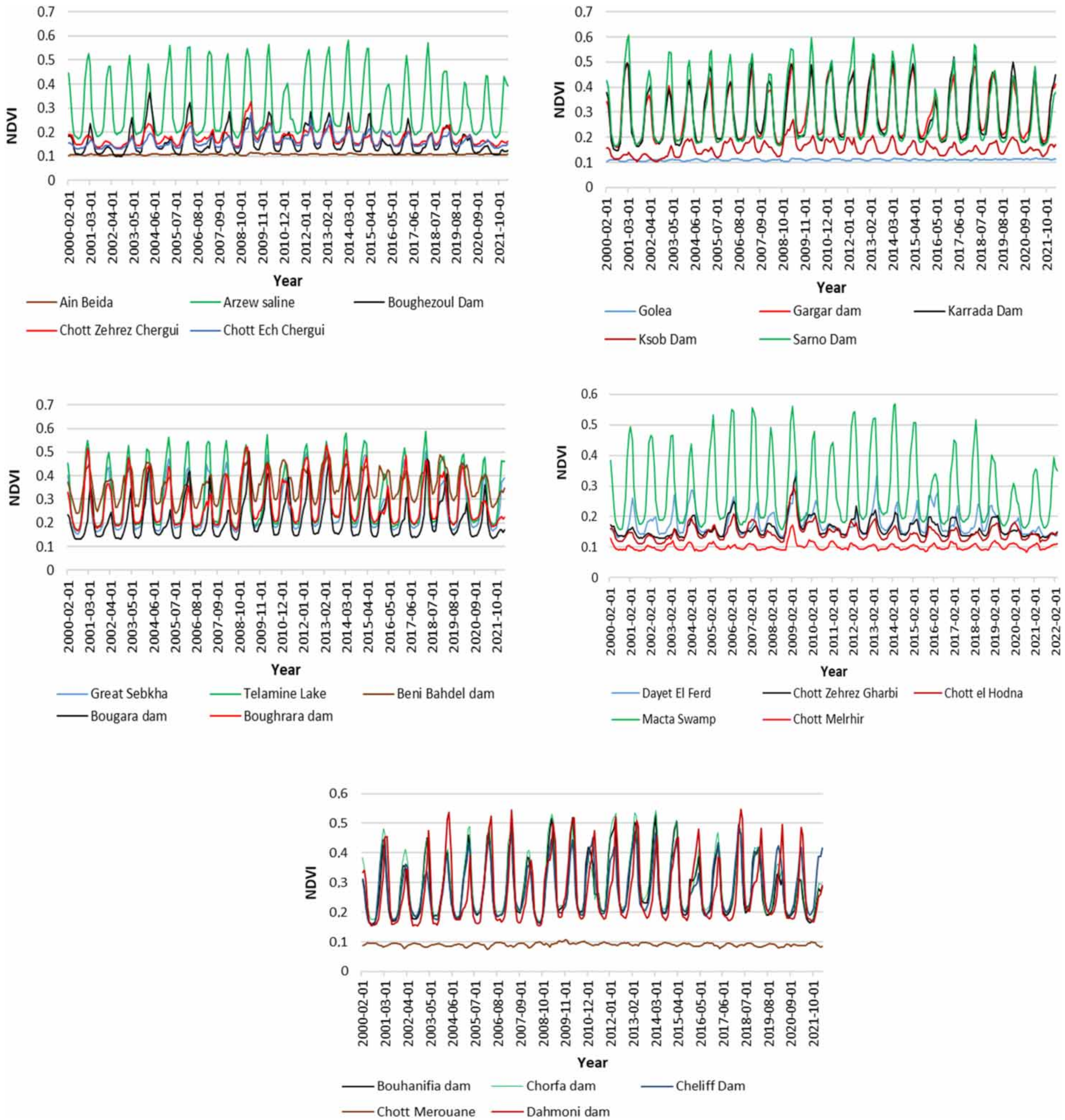

Figure 2 | The pattern of interannual changes in the annual average NDVI for 25 watersheds in Algeria over the period of 2000 to 2022.

Conversely, areas from Ksob dam off the southern saline of Golea had the lowest average NDVI, measuring 0.05. These areas were predominantly classified as having moderate to low or low vegetation cover, suggesting sparse vegetation and unfavorable environmental conditions. Hence, there is a need for implementing appropriate measures to increase green spaces in these regions. The average NDVI for Boughezoul dam, Chott Zehrez Chergui, Chott Ech Chergui, Chott Zehrez Gharbi, and Dayet El Ferd ranged from 0.2 to 0.4, indicating relatively low vegetation cover. These basins can be categorized as medium/low vegetation areas with a very poor vegetation condition.

3.2. Spatio-temporal variation of NDVI, EVI, NDWI, and LST

The four remote sensing indicators (NDVI, NDWI, EVI, and LST) have been calculated using average values obtained from the NIR and SWIR (short-wave infrared) bands of the MODIS datasets. The annual average values of these indicators from 2000 to 2022 show that the NDWI values were comparatively low throughout the study timeframe, varying from 0.07 to −0.2 across all study sites (Figure 3). The mean values of the NDVI varied from 0 to 0.7. The highest NDVI values were observed in the northwest regions. The EVI ranged from 0.06 to 0.41, with the highest value of 0.41 recorded in the Sarno and Ksob basins in 2012 and the Macta basin in 2014. The lowest value, 0.066, was observed in Chott Merouane in 2006 (Figure 4). The mean LST in all study areas ranged from 13°C to 18°C. Despite variations in location and land characteristics, there were no discernible discrepancies in surface temperatures. The highest surface temperatures were recorded in the southern regions (Figure 5).

3.3. The associations between NDVI and LST

Generally, a consistent negative association is observed between NDVI and LST, as depicted in Figure 6. This negative correlation spans the entire study area. Specific regions, including Macta Marsh, Arzew saline, Great Sebkha, Chott Melrhir, Beni Bahdel dam, Cheliff dam, Chorfa dam, Bouhanfia dam, Karrada dam, Gargar dam, and Telamine Lake, exhibit a moderate negative relationship between NDVI and LST. The corresponding average R^2 values for these regions are 0.5701, 0.5637, 0.5323, 0.4262, 0.4661, 0.4543, 0.4161, 0.4351, 0.4188, 0.48, and 0.5635, respectively. This suggests that changes in LST are moderately associated with variations in vegetation, with a tendency for NDVI to decline as LST rises in these regions.

In other regions, a strong negative relationship between NDVI and LST has decreased over time. The R^2 values in these areas range from 0.109 to 0.3793. This indicates that as LST values increase, there is a corresponding decrease in vegetation. The negative relationship between NDVI and LST suggests that higher temperatures are linked to reduced vegetation activity in these regions. It is essential to note that the connection between NDVI and LST differs for water bodies. In the case of

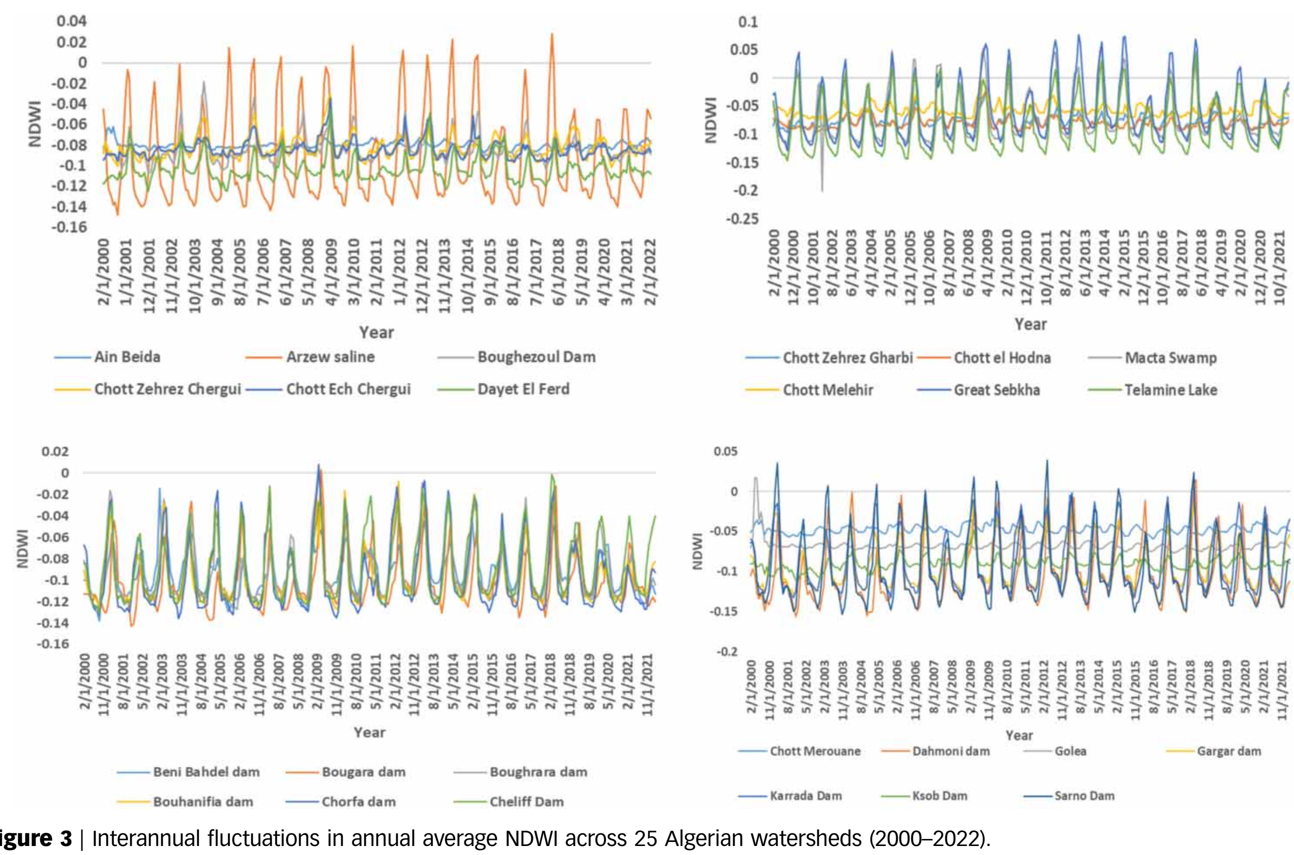

Figure 3 | Interannual fluctuations in annual average NDWI across 25 Algerian watersheds (2000–2022).

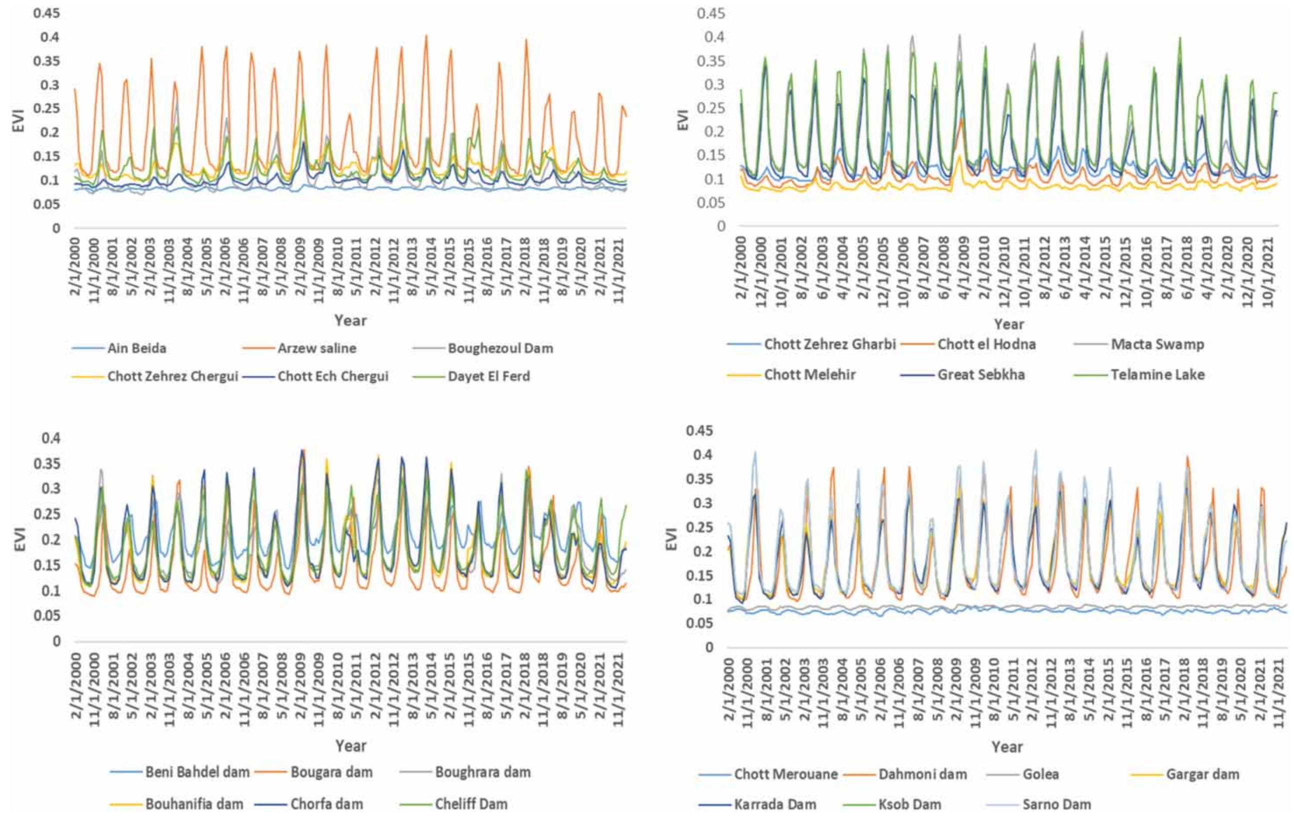

Figure 4 | Interannual fluctuations in annual average EVI across 25 Algerian watersheds (2000–2022).

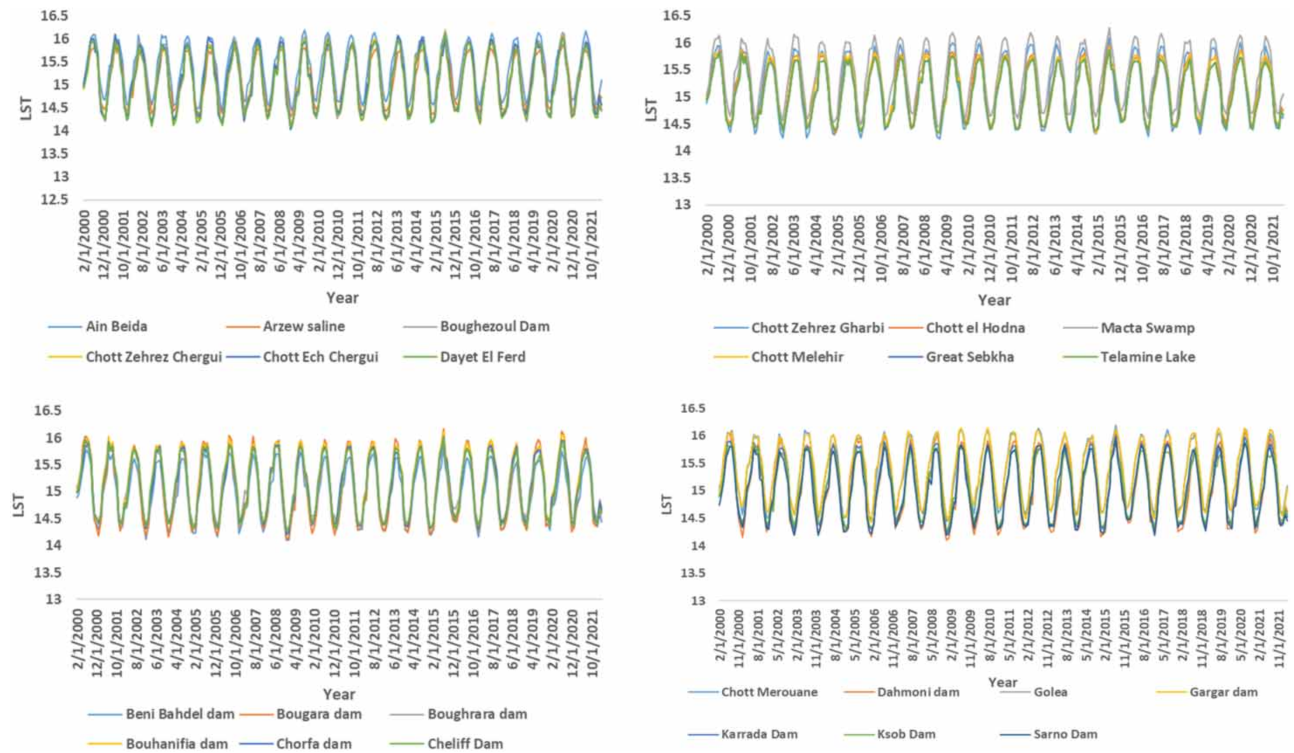

Figure 5 | Interannual fluctuations in annual average LST across 25 Algerian watersheds (2000–2022).

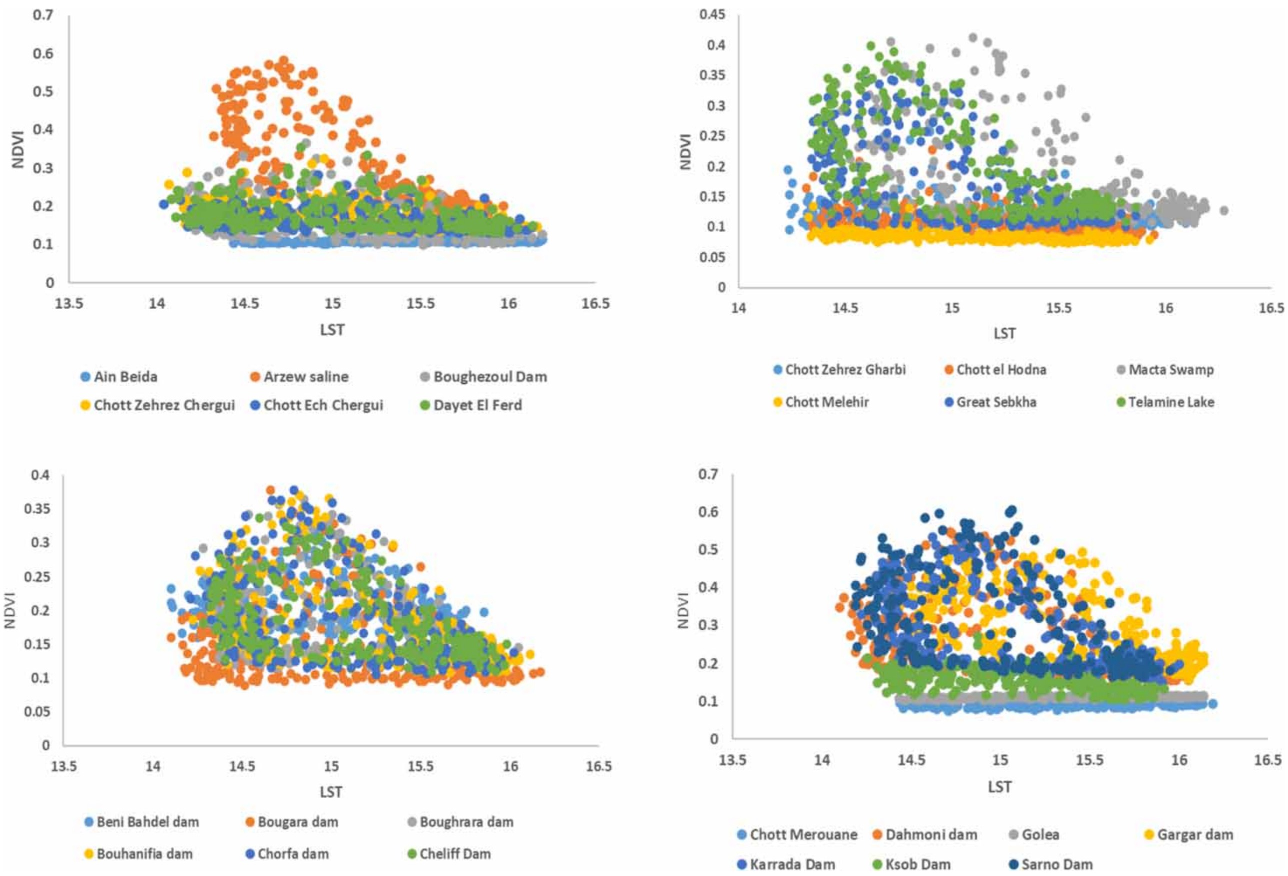

Figure 6 | Annual assessment of relationship between NDVI and LST indices during 2000–2022.

water bodies or wetlands, a negative NDVI indicates the presence of water. The wave-like pattern observed between NDVI and LST for water bodies may be influenced by variables such as water level and temperature.

Overall, the observed relationships between NDVI and LST provide valuable insights into the dynamics of vegetation and LST in the study site. These findings are crucial for understanding the impact of temperature on vegetation health and for monitoring environmental changes over time.

3.4. Mann–Kendall analysis trends

The MK analysis was performed on the NDVI, EVI, NDWI, and LST datasets at a 95% confidence level, with serial correlation applied. The results of the MK test for the NDVI data are summarized in Table 3. Among the 25 regions examined, 15 displayed negative MK statistics, indicating an overall decreasing trend in NDVI over the study period. The associated *p*-values for these regions exceeded the specified significance level (alpha), indicating significant evidence of a monotonic decline in vegetation activity within these areas.

In contrast, the MK analysis revealed a positive slope for the remaining ten regions, indicating a general increasing trend in NDVI. The positive values of the statistic were relatively high, providing additional support for the presence of a significant upward pattern. The *p*-values associated with these regions were lower than the specified significance level (alpha), indicating strong evidence of a monotonic increasing trend in vegetation activity within these areas (Figure 7). It is noteworthy that each region's *p*-value was either greater than or less than 0.05, serving as the threshold for statistical significance. These results provide insights into the direction and significance of trends in vegetation indices across the study regions.

The MK test outcomes for EVI, outlined in Table 4, mirrored the NDVI results in the majority of regions, suggesting a similar trend. However, an exception was noted in the Ksob region, where the EVI trend displayed a distinct positive direction, signifying an overall increase in vegetation activity. The *p*-value associated with this region was lower than the specified

Table 3 | Findings of the two-tailed test for seasonality in the NDVI time series using the MK method

Study areas	tau	*p*-value	Sen's slope
Ain Beida	0.167	0.00013	0.0004
Arzew saline	0.016	0.700	0.006
Boughezoul dam	−0.007	0.871	0.005
Chott Zehrez Chergui	0.014	0.732	0.000
Chott Ech Chergui	0.136	0.001	0.006
Dayet El Ferd	−0.029	0.480	−0.001
Chott Zehrez Gharbi	0.021	0.621	0.002
Chott El Hodna	0.009	0.829	−0.001
Macta Marsh	−0.028	0.490	0.004
Chott Melrhir	0.088	0.036	0.000
Great Sebkha	0.049	0.234	0.004
Telamine Lake	0.053	0.203	0.004
Beni Bahdel dam	0.127	0.002	0.017
Bougara dam	0.070	0.091	0.007
Boughrara dam	0.049	0.239	0.014
Bouhanifia dam	0.052	0.208	0.014
Chorfa dam	0.024	0.560	0.009
Cheliff dam	0.138	0.001	0.012
Chott Merouane	−0.047	0.262	0.000
Dahmoni dam	0.092	0.026	0.007
Golea	0.344	<0.0001	0.001
Gargar dam	0.114	0.006	0.012
Karrada dam	0.089	0.031	0.002
Ksob dam	0.162	<0.0001	0.005
Sarno dam	−0.002	0.960	−0.001

significance level (alpha), providing strong evidence of a significant monotonic upward trend in vegetation activity in the Ksob region (Figure 7).

In NDWI, positive values observed in 18 regions suggest an increasing trend in water content. The corresponding *p*-values (>0.05) for these regions indicate a monotonically positive trend. Conversely, other regions with *p*-values below 0.05 show a significant negative trend in water content. MK test results provide evidence of monotonic trends, either increasing or decreasing, in NDWI values across the study regions (Figure 7).

The application of long-term sequence analysis (LST) with the MK test provides results from the statistical trend analysis of annual temperature degrees, as outlined in Table 6. These findings reveal a statistically significant positive trend in all wetlands, indicating a gradual increase over time. The analysis suggests a substantial alteration in annual temperature magnitudes, particularly between the years 2020 and 2022. The confirmed results, based on the MK statistics and accompanying *p*-values at significance levels of 5% and 1%, demonstrate statistical significance (Figure 7). As anticipated, both variables representing the maximum temperature show a consistent upward trend. In summary, the findings of the trend test demonstrate a statistically significant pattern of temperature rise in all regions.

Sen's slope was utilized to analyze time-series data of natural indicators from 2020 to 2022 (Tables 3–6). In all scenarios, the indicators exhibited a noticeable and continuous upward trend. There was an increase in vegetation density based on NDVI and EVI values in Beni Bahdel dam, Bouhanifia dam, Boughrara dam, and Gargar dam. Additionally, NDWI analysis indicated an increase in water content in Ksob dam, Boughezoul dam, and Chott Zehrez Gharbi. The rise in surface temperature over time suggests environmental conditions characterized by excessive heat, which may negatively impact vegetation density.

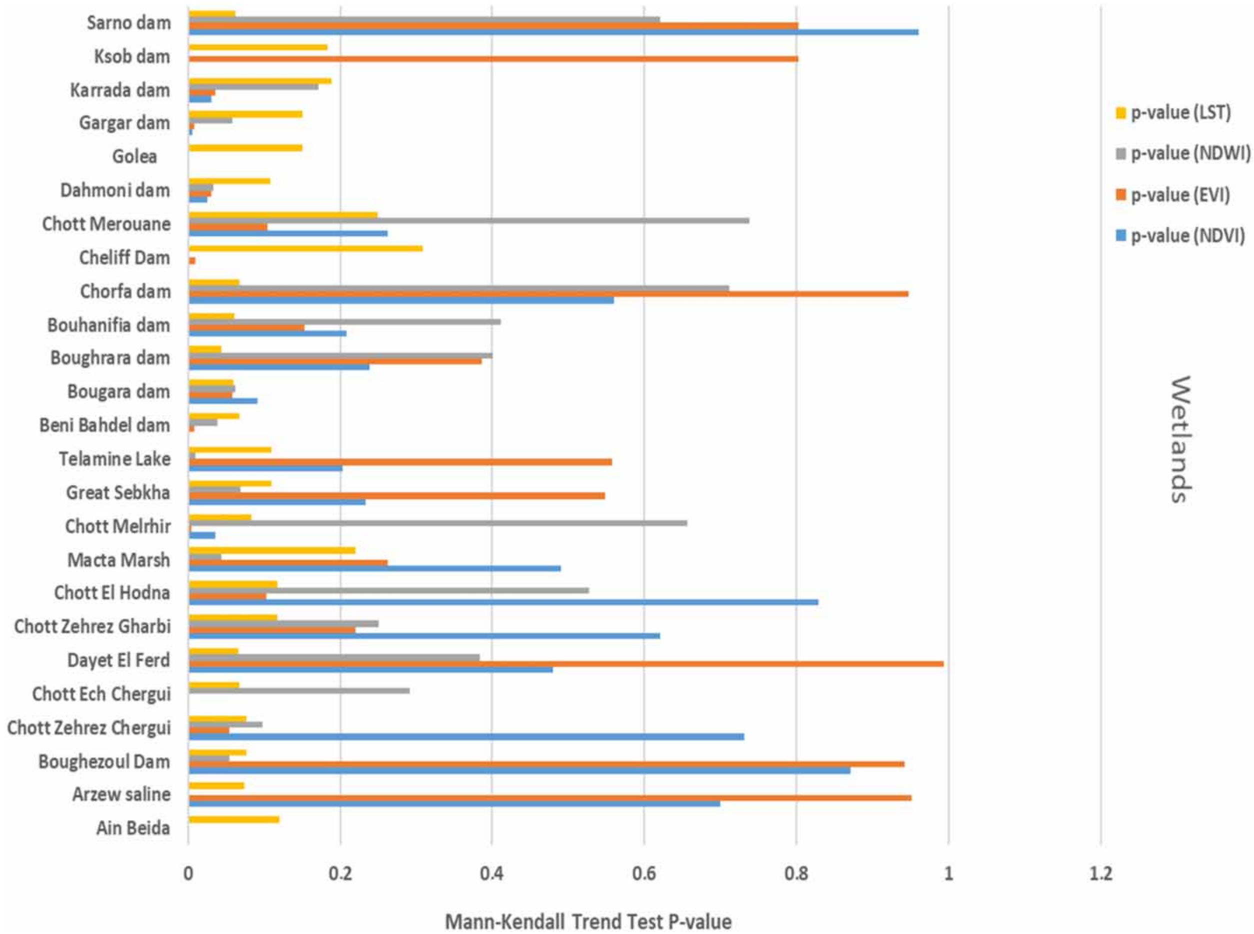

Figure 7 | MK trend test for annual NDVI, EVI, NDWI, LST, 2020–2022.

The results of the Sen's slope analysis revealed that the most affected areas in terms of vegetation cover are Dayet El Ferd, Sarno dam, Chott El Hodna, Ain Beida, Arzew Saline, Chott Ech Chergui, Telamine Lake, Chott Merouane, Golea, Gargar dam, Karrada dam, and Sarno dam. The trend test results, with a significance level of 1%, showed statistically significant trends for the indicators, with the results remaining statistically significant at a 95% confidence level from 2020 to 2022.

3.5. Discussion

The primary aim of this study was to assess fluctuations in the NDVI and variations in water bodies over the past 22 years. Long-term monitoring of vegetation and the analysis of influential factors are crucial components of studying global changes (Jin *et al.* 2020). The study findings indicate a significant decrease in NDVI datasets over time (Figure 2). The NDVI values ranged between 0 and 0.7 and were compared with higher and lower values in multi-temporal datasets. In the Chott Merouane region, 2006 exhibited the most negative NDVI values. Several regions also experienced a significant deterioration in vegetation, with values not exceeding 0.2. Additionally, lower healthy vegetation with higher NDVI values was observed due to lower vegetation density. These findings suggest a history of drought and plant stress in these areas. However, certain regions showed an overall rise in NDVI values, surpassing 0.4. The highest NDVI levels in the Sarno watershed were recorded in 2001 (>0.6), indicating abundant vegetation and healthy green spaces. Nevertheless, these same regions have witnessed a substantial decline in vegetation over the years, potentially due to factors such as drought and climatic conditions.

The study findings reveal that the EVI vegetation indicators exhibited stronger spatio-temporal correlations in the study area. While NDVI showed higher values compared with EVI and NDWI, it did not demonstrate a significant relationship with LST based on the obtained results. EVI, on the other hand, emerged as the second-best indicator with a more robust interconnection. This could be attributed to the sensitivity of the EVI to the spectral impact of soil composition and moisture

Table 4 | Findings of the two-tailed test for seasonality in the EVI time series using the MK method

Study areas	tau	*p*-value	Sen's slope
Ain Beida	0.142	0.001	0.0002
Arzew saline	−0.003	0.951	0.002
Boughezoul dam	−0.003	0.942	0.002
Chott Zehrez Chergui	0.080	0.055	0.002
Chott Ech Chergui	0.199	<0.0001	0.002
Dayet El Ferd	0.000	0.993	−0.001
Chott Zehrez Gharbi	0.051	0.220	0.001
Chott El Hodna	0.068	0.103	0.001
Macta Marsh	−0.046	0.262	0.000
Chott Melrhir	0.121	0.004	0.001
Great Sebkha	0.025	0.548	−0.002
Telamine Lake	0.024	0.558	−0.002
Beni Bahdel dam	0.109	0.008	0.005
Bougara dam	0.079	0.058	0.002
Boughrara dam	0.036	0.387	0.007
Bouhanifia dam	0.059	0.153	0.004
Chorfa dam	0.003	0.947	0.000
Cheliff dam	0.107	0.010	0.000
Chott Merouane	0.069	0.105	0.006
Dahmoni dam	0.089	0.031	0.001
Golea	0.301	<0.0001	0.005
Gargar dam	0.109	0.008	0.002
Karrada dam	0.086	0.036	0.005
Ksob dam	0.010	0.803	0.005
Sarno dam	0.010	0.803	0.000

in areas with limited vegetation coverage (Lu *et al.* 2015). In this research, the weak relationship between NDVI and LST could be due to several factors. NDVI primarily captures the greenness of vegetation and may not directly reflect the thermal properties of the land surface. Additionally, other factors such as soil type, moisture content, and land cover composition can influence the association between NDVI and LST.

The MK test was employed to examine trends in the chronological datasets of NDVI, EVI, NDWI, and LST in the 25 wetlands. The *p*-value emerges as a critical outcome, providing insights into the significance of the data, the presence of a trend, and whether that trend is monotonous (Guo *et al.* 2018).

The analysis of NDVI, EVI, NDWI, and LST datasets revealed diverse trends due to their distinct values. The MK test demonstrated a significant monotonically decreasing trend in NDVI ($p < 0.05$). EVI values, ranging from 0.0001 to 0.951, generally mirrored the NDVI and NDWI results in specific wetlands such as Ain Beida, Chott Ech Chergui, Chott Melrhir, Beni Bahdel dam, Cheliff dam, Dahmoni dam, Golea, Gargar dam, Karrada dam, and Ksob dam. In contrast, these areas with decreasing trends are exacerbating water stress, leading to water deficits and reduced vegetation activity.

On the other hand, the NDVI, EVI, and NDWI values were positive in wetlands such as Arzew saline, Boughezoul dam, Chott Zehrez Chergui, Dayet El Ferd, Chott Zehrez Gharbi, Chott El Hodna, Macta Marsh, Great Sebkha, Telamine Lake, Bougara dam, Boughrara dam, Bouhanifia dam, Chorfa dam, Chott Merouane, and Sarno dam, indicating a positive trend across all datasets. To determine whether the trend is monotonous, a *p*-value less than 0.05 is considered. The MK test for LST showed that in all wetland regions with a positive monotonous trend, there was a consistently ascending pattern, indicating an undiminished trend (Royden & Fitzpatrick 2010). The presence of a non-monotonous trend suggests fluctuations of

Table 5 | Findings of the two-tailed test for seasonality in the NDWI time series using the MK method

Study areas	Tau	*p*-Value	Sen slope
Ain Beida	0.028	0.0521	−0.0001
Arzew Saline	0.050	0.227	−0.002
Boughezoul dam	0.080	0.055	0.001
Chott Zehrez Chergui	0.069	0.098	0.0001
Chott Ech Chergui	−0.044	0.292	−0.001
Dayet El Ferd	0.036	0.384	0.0002
Chott Zehrez Gharbi	0.048	0.251	0.001
Chott El Hodna	−0.026	0.527	0.000
Macta Swamp	0.083	0.044	0.003
Chott Melrhir	0.019	0.657	0.0003
Great Sebkha	0.075	0.069	0.006
Telamine Lake	0.106	0.010	−0.0004
Beni Bahdel dam	0.086	0.038	0.005
Bougara dam	0.078	0.062	0.001
Boughrara dam	0.035	0.401	0.001
Bouhanifia dam	0.034	0.412	0.001
Chorfa dam	0.015	0.712	0.002
Cheliff dam	0.134	0.001	0.001
Chott Merouane	0.014	0.738	−0.001
Dahmoni dam	0.088	0.034	0.006
Golea	−0.132	0.002	−0.001
Gargar dam	0.079	0.058	−0.0006
Karrada dam	0.057	0.171	−0.0001
Ksob dam	0.153	0.0001	0.002
Sarno dam	−0.020	0.621	−0.001

both increasing and decreasing trends over the years, indicating variable responses to drought conditions and higher water deficits in different areas. In contrast, the remaining wetland regions displayed a consistent, monotonous trend throughout the entire period.

Examining Sen's slope on time-series data spanning from 2020 to 2022, with a specific emphasis on natural indicators, yields significant knowledge regarding the environmental changes occurring in various wetlands. The results emphasize notable patterns and alterations in the density of vegetation, moisture level, and surface temperature in different geographical areas. The evident and consistent rising trajectory in vegetation density, as evidenced by NDVI and EVI values, suggests favorable ecological transformations. The reported increase was noted in multiple dams, namely Beni Bahdel dam, Bouhanifia dam, Boughrara dam, and Gargar dam. The increase in vegetation density suggests enhanced environmental conditions and may have favorable consequences for biodiversity and ecological well-being in these regions.

The NDWI research has detected a significant rise in the water content of Ksob dam, Boughezoul dam, and Chott Zehrez Gharbi, which is an important observation. This implies fluctuations in water accessibility, which could possibly affect aquatic habitats and the surrounding environment. It is crucial to monitor these changes to comprehend the water dynamics and guarantee sustainable management of water resources.

The progressive increase in surface temperature over a period of time, suggesting climatic circumstances typified by an excessive amount of heat, is a worrisome pattern. High temperatures can negatively impact the density of vegetation, perhaps resulting in decreased biodiversity and modified ecosystems. This discovery highlights the significance of tackling climate-related difficulties and executing plans for climate resilience.

Table 6 | Findings of the two-tailed test for seasonality in the LST time series using the MK method

Study areas	tau	*p*-value	Sen's slope
Ain Beida	0.056	0.120	0.023
Arzew saline	0.068	0.074	0.010
Boughezoul dam	0.068	0.077	0.040
Chott Zehrez Chergui	0.068	0.077	0.063
Chott Ech Chergui	0.072	0.067	0.044
Dayet El Ferd	0.072	0.066	0.053
Chott Zehrez Gharbi	0.056	0.117	0.045
Chott El Hodna	0.056	0.117	0.017
Macta Swamp	0.036	0.221	0.028
Chott Melrhir	0.064	0.083	0.013
Great Sebkha	0.060	0.110	0.003
Telamine Lake	0.060	0.110	0.003
Beni Bahdel dam	0.072	0.067	0.002
Bougara dam	0.072	0.060	0.006
Boughrara dam	0.084	0.044	0.005
Bouhanifia dam	0.072	0.061	0.009
Chorfa dam	0.072	0.067	0.014
Cheliff dam	0.024	0.309	0.007
Chott Merouane	0.032	0.249	0.038
Dahmoni dam	0.056	0.109	0.000
Golea	0.048	0.151	0.021
Gargar dam	0.048	0.151	0.021
Karrada dam	0.040	0.189	0.006
Ksob dam	0.044	0.183	0.022
Sarno dam	0.076	0.062	0.040

The areas with the highest impact on vegetation cover, namely Dayet El Ferd, Sarno dam, Chott El Hodna, Ain Beida, Arzew saline, Chott Ech Chergui, Telamine Lake, Chott Merouane, Golea, Gargar dam, Karrada dam, and Sarno dam, have been identified as key areas for targeted conservation and environmental management efforts. Gaining a comprehensive understanding of the particular obstacles encountered by these locations is essential for adopting efficient mitigation strategies.

The statistical significance of the trend test results, with a significance threshold of 1%, enhances the reliability of the findings. The continued presence of statistically significant trends, with a confidence level of 95%, from 2020 to 2022 highlights the strength and reliability of the observed changes. This knowledge holds significant value for policymakers and researchers as it enables them to make well-informed decisions on environmental conservation and resource management techniques.

Ultimately, the Sen's slope analysis of time-series data has revealed significant patterns and fluctuations in environmental indicators across different dams and locations. These findings establish a basis for focused environmental interventions, highlighting the importance of sustainable practices and adaptable techniques to tackle the difficulties presented by shifting environmental conditions. Continual surveillance and investigation will be crucial to assess the enduring effects and improve conservation strategies accordingly.

4. CONCLUSIONS

The comprehensive analysis conducted in this study utilizes an extensive dataset of NDVI spanning from 2000 to 2022 to examine changes in 25 different regions over a period of 22 years. The average mean NDVI values varied from 0 to 0.7, with a mean percentage between 0.098% and 0.34%. The analysis revealed a noticeable decline in NDVI values over the course of the multi-year cycle. Additionally, many regions exhibited significant deterioration in vegetation, with values not exceeding 0.2.

The study found that NDVI had a stronger spatial and temporal response compared with EVI. The correlation between NDVI and EVI was also notable, contributing to the overall findings. The negative association between NDVI and LST underscores the impact of drought and plant stress on vegetation in the study areas ($R^2 = 0.109$ to $R^2 = 0.5701$). The significant negative correlations between NDVI and LST values indicate that higher temperatures are associated with reduced vegetation density and health.

The findings derived from the MK trend analysis underscore the importance of NDVI, highlighting its strong association with EVI. Overall, the findings of this study emphasize the severity of the changes and degradation observed in these areas, which can be attributed to factors such as droughts and other climatic conditions that induce stress on vegetation.

These findings provide valuable information for understanding the dynamics of vegetation and water stress, highlighting the need for effective management and conservation measures in the studied regions.

DATA AVAILABILITY STATEMENT

All relevant data are included in the paper or its Supplementary Information.

CONFLICT OF INTEREST

The authors declare there is no conflict.

REFERENCES

Belgherbi, B. & Benabdeli, K. 2010 Contribution à l'étude des causes de dégradation de la forêt de Tamarix de la zone humide de la Macta (Algérie occidentale). *Forêt méditerranéenne* **XXXI**, 55–62.

Ben Salem, S., Ben Salem, A., Karmaoui, A., Yacoubi, M. K. & Messouli, M. 2019 Quantification and evaluation of water erosion: application of the model SDR–InVEST in the Ziz basin in south-east Morocco. In: *Decision Support Methods for Assessing Flood Risk and Vulnerability* (Karmaoui, A., ed.), IGI Global, Hershey, PA, USA, pp. 140–161. doi:10.4018/978-1-5225-9771-1.ch007.

Chen, X., Zhao, H., Li, P. & Yin, Z. 2006 Remote sensing image-based analysis of the relationship between urban heat island and land use/cover changes. *Remote Sensing of Environment* **104**, 133–146.

Davidson, N. C. 2014 How much wetland has the world lost? Long-term and recent trends in global wetland area. *Mar. Freshw. Res.* **65**, 934–941. doi:10.1071/MF14173.

De Jong, R., de Bruin, S., de Wit, A., Schaepman, M. E. & Dent, D. L. 2011 Analysis of monotonic greening and browning trends from global NDVI time-series. *Remote Sens. Environ.* **115** (2), 692–702. doi:10.1016/j.rse.2010.10.011.

DGF (Directorate General of Forests) 2017 *Inventaire des Zones Humides en Algérie*. Report, DGF, Algeria.

Donohue, I., Hillebrand, H., Montoya, J. M., Petchey, O. L., Pimm, S. L., Fowler, M. S., Healy, K., Jackson, A. L., Lurgi, M., McClean, D., O'Connor, N. E., O'Gorman, E. J. & Yang, Q. 2016 Navigating the complexity of ecological stability. *Ecology Letters* **19**, 1172–1185.

Gajbhiye, S., Meshram, C., Singh, S. K., Srivastava, P. K. & Islam, T. 2016 Precipitation trend analysis of Sindh River basin, India, from 102-year record (1901–2002). *Atmos. Sci. Lett.* **17**, 71–77. doi:10.1002/asl.602.

Ghodbani, T. & Amokrane, K. 2013 La zone humide de la Macta: un espace à protéger sur le littoral ouest de l'Algérie. *Rev. Physio-Géo* **7**, 139–155.

Gorelick, N., Hancher, M., Dixon, M., Ilyushchenko, S., Thau, D. & Moore, R. 2017 Google Earth Engine: planetary-scale geospatial analysis for everyone. *Remote Sens. Environ.* **202**, 18–27. doi:10.1016/j.rse.2017.06.031.

Guo, M., Li, J., He, H., Xu, J. & Jin, Y. 2018 Detecting global vegetation changes using Mann-Kendal (MK) trend test for 1982–2015 time period. *Chin. Geogr. Sci.* **28** (6), 907–919. doi: 10.1007/s11769-018-1002-2.

Guo, E., Wang, Y., Wang, C., Sun, Z., Bao, Y., Mandula, N., Jirigala, B., Bao, Y. & Li, H. 2021 NDVI indicates long-term dynamics of vegetation and its driving forces from climatic and anthropogenic factors in Mongolian plateau. *Remote Sens.* **13** (4), 688. doi:10.3390/rs13040688.

Hu, Y., Dao, R. & Hu, Y. 2019 Vegetation change and driving factors: contribution analysis in the Loess Plateau of China during 2000–2015. *Sustainability* **11**, 1320. doi:10.3390/su11051320.

Hua, J. W., Zhu, S. Y. & Zhang, G. X. 2018 Downscaling land surface temperature based on random forest algorithm. *Remote Sens. Land Resour.* **30**(1), 78–86. doi:10.6046/gtzyyg.2018.01.11.

Huang, S., Tang, L., Hupy, J. P., Wang, Y. & Shao, G. 2020 A commentary review on the use of normalized difference vegetation index (NDVI) in the era of popular remote sensing. *J. For. Res.* **32**, 1–6. doi:10.1007/s11676-020-01155-1.

Huete, A., Justice, C. & Liu, H. 1994 Development of vegetation and soil indices for MODIS-EOS. *Remote Sens. Environ.* **49**, 224–234. doi:10.1016/0034-4257(94)90018-3.

Huete, A. R., Liu, H. Q., Batchily, K. & van Leeuwen, W. 1997 A comparison of vegetation indices over a global set of TM images for EOS-MODIS. *Remote Sens. Environ.* **59** (3), 440–451. doi:10.1016/S0034-4257(96)00112-5.

IPCC 2023 Sections 1–4. In: *Climate Change 2023: Synthesis Report. Contribution of Working Groups I, II and III to the Sixth Assessment Report of the Intergovernmental Panel on Climate Change* (Core Writing Team, Lee, H. & Romero, J., eds), IPCC, Geneva, Switzerland, pp. 35–115. doi:10.59327/IPCC/AR6-9789291691647.

Jin, K., Wang, F., Han, J., Shi, S. & Ding, W. 2020 Contribution of climatic change and human activities to vegetation NDVI change over China during 1982–2015. *Acta Geogr. Sin.* **75** (5), 961–974. doi:10.11821/dlxb202005006.

Karl, T. R. & Trenberth, K. E. 2003 Modern global climate change. *Science* **302** (5651), 1719–1723. doi:10.1126/science.1090228.

Kendall, M. G. 1975 *Rank Correlation Methods.* Griffin, London, UK.

Keria, H., Bensaci, E. & Zoubiri, A. 2023 Monitoring the effect of droughts and extreme climate variables for various time periods on vegetation density in the Reghaia catchment, Algeria. *Nat. Resou. Sustain. Dev.* **13** (1), 119–136. doi:10.31924/nrsd.v13i1.122.

Kong, D., Miao, C., Wu, J., Zheng, H. & Wu, S. 2020 Time lag of vegetation growth on the Loess Plateau in response to climate factors: estimation, distribution, and influence. *Sci. Total Environ.* **744**, 140726. doi:10.1016/j.scitotenv.2020.140726.

Koopmanschap, E. M. J., Hammami, M. & Klok, T. C. 2011 *Lac Ayata dans la Vallée d'Oued Righ. Quick-scan of Options and Preliminary Recommendations for the Management of Lake Ayata in the Valley of Oued Righ.* Centre for Development Innovation, Wageningen University & Research Centre, Wageningen, The Netherlands.

Kumar, S., Machiwal, D. & Dayal, D. 2017 Spatial modelling of rainfall trends using satellite datasets and geographic information system. *Hydrol. Sci. J.* **62**, 1636–1653. doi:10.1080/02626667.2017.1304643.

Lu, L., Kuenzer, C., Wang, C., Guo, H. & Li, Q. 2015 Evaluation of three MODIS-derived vegetation index time series for dryland vegetation dynamics monitoring. *Remote Sens.* **7**, 7597–7614. doi:10.3390/rs70607597.

Mann, H. B. 1945 Nonparametric tests against trend. *Econometrica* **13**, 245–259. doi:10.2307/1907187.

McFeeters, S. K. 1996 The use of the Normalized Difference Water Index (NDWI) in the delineation of open water features. *Int. J. Rem. Sens.* **17** (7), 1425–1432. doi:10.1080/01431169608948714.

Megharbi, A., Abdoun, F. & Belgherbi, B. 2016 Diversité floristique en relation avec les gradients abiotiques dans la zone humide de la Macta (ouest d'Algérie). *Revue d'Ecologie (Terre et Vie)* **71** (2), 142–155.

Moumane, A., El Ghazali, F. E., Al Karkouri, J., Delorme, J., Batchi, M., Chafiki, D. & Karmaoui, A. 2021 Monitoring spatiotemporal variation of groundwater level and salinity under land use change using integrated field measurements, GIS, geostatistical, and remote-sensing approach: case study of the Feija aquifer, Middle Draa watershed, Moroccan Sahara. *Environ. Monit. Assess.* **193**, 769. doi:10.1007/s10661-021-09581-2.

Myneni, R. B., Hall, F. G., Sellers, P. J. & Marshak, A. L. 1995 The interpretation of spectral vegetation indexes. *IEEE Trans. Geosci. Remote Sens.* **33** (2), 481–486. doi:10.1109/TGRS.1995.8746029.

Myneni, R. B., Keeling, C. D., Tucker, C. J., Asrar, G. & Nemani, R. R. 1997 Increased plant growth in the northern high latitudes from 1981 to 1991. *Nature* **386**, 698–702. doi:10.1038/386698a0.

Nagendra, H., Lucas, R., Honrado, J. P., Jongman, R. H. G., Tarantino, C., Adamo, M. & Mairota, P. 2013 Remote sensing for conservation monitoring: assessing protected areas, habitat extent, habitat condition, species diversity, and threats. *Ecol. Indic.* **33**, 45–59. doi:10.1016/j.ecolind.2012.09.014.

Nanzad, L., Zhang, J., Tuvdendorj, B., Nabil, M., Zhang, S. & Bai, Y. 2019 NDVI anomaly for drought monitoring and its correlation with climate factors over Mongolia from 2000 to 2016. *J. Arid Environ.* **164**, 69–77. doi:10.1016/j.jaridenv.2019.01.019.

Nedkov, S., Zhiyanski, M., Borisova, B., Nikolova, M., Bratanova-Doncheva, S., Semerdzhieva, L., Ihtimanski, I., Nikolov, P. & Aidarova, Z. 2018 A geospatial approach to mapping and assessment of urban ecosystem services in Bulgaria. *Eur. J. Geogr.* **9** (4), 34–50.

Nemani, R. R., Keeling, C. D., Hashimoto, H., Jolly, W. M., Piper, S. C., Tucker, C. J., Myneni, R. B. & Running, S. W. 2003 Climate-driven increases in global terrestrial net primary production from 1982 to 1999. *Science* **300**, 1560–1563. doi:10.1126/science.1082750.

Noorisameleh, Z., Khaledi, S., Shakiba, A., Firouzabadi, P. Z., Gough, W. A. & Mirza, M. M. Q. 2020 Comparative evaluation of impacts of climate change and droughts on river flow vulnerability in Iran. *Water Sci. Eng.* **13** (4), 265–274. doi:10.1016/j.wse.2020.05.001.

O'Connor, B., Secades, C., Penner, J., Sonnenschein, R., Skidmore, A., Burgess, N. D. & Hutton, J. M. 2015 Earth observation as a tool for tracking progress towards the Aichi Biodiversity Targets. *Remote Sens. Ecol. Conserv.* **1**, 19–28. doi:10.1002/rse2.4.

Ougougdal, H. A., Khebiza, M. Y., Messouli, M., Bounoua, L. & Karmaoui, A. 2020 Delineation of vulnerable areas to water erosion in a mountain region using SDR–InVEST model: a case study of the Ourika watershed, Morocco. *Sci. Afr.* **10**, e00646. doi:10.1016/j.sciaf.2020.e00646.

Piao, S., Fang, J., Zhou, L., Guo, Q., Henderson, M., Ji, W., Li, Y. & Tao, S. 2003 Interannual variations of monthly and seasonal normalized difference vegetation index (NDVI) in China from 1982 to 1999. *J. Geophys. Res.* **108**, 4401. doi:10.1029/2002JD002848.

Piao, S. L., Wang, X. H., Ciais, P., Zhu, B., Wang, T. & Liu, J. 2011 Changes in satellite-derived vegetation growth trend in temperate and boreal Eurasia from 1982 to 2006. *Glob. Change Biol.* **17**, 3228–3239. doi:10.1111/j.1365-2486.2011.02419.x.

Pingale, S. M., Khare, D., Jat, M. K. & Adamowski, J. 2016 Trend analysis of climatic variables in an arid and semi-arid region of the Ajmer District, Rajasthan, India. *J. Water Land Dev.* **28**, 3–18. doi:10.1515/jwld-2016-0001.

Potter, C., Tan, P.-N., Steinbach, M., Klooster, S., Kumar, V., Myneni, R. & Genovese, V. 2003 Major disturbance events in terrestrial ecosystems detected using global satellite data sets. *Glob. Change Biol.* **9**, 1005–1021. doi:10.1046/j.1365-2486.2003.00648.x.

Ramsar 2001 Marais de la Macta, Grand Sebkha, Chott El Hodna, Chott Ech Chergui. Ramsar Sites Information Service (Algeria). https://rsis.ramsar.org/ris/1059.

Ramsar 2002 Chott Melghir. Ramsar Sites Information Service (Algeria). https://rsis.ramsar.org/ris/1296.

Ramsar 2003 Chott de Zehrez Chergui. Ramsar Sites Information Service (Algeria). https://rsis.ramsar.org/ris/1294.

Ramsar 2004 Instrument de planification nationale pour l'application des dispositions de la Convention de Ramsar sur les zones humides. Ramsar Convention (Algeria).

Ramsar 2011 Lac du barrage de Boughezoul. Ramsar Sites Information Service (Algeria). https://rsis.ramsar.org/ris/1960.

Ramsar 2015 La Convention de Ramsar: qu'est-ce que c'est? https://www.ramsar.org/sites/default/files/documents/library/fs_6_ramsar_convention_fr.pdf.

Royden, H. & Fitzpatrick, P. 2010 *Real Analysis*. 4th edn. Pearson, New York, USA.

Sen, P. K. 1968 Estimates of the regression coefficient based on Kendall's tau. *J. Am. Stat. Assoc.* **63** (324), 1379–1389. doi:10.1080/01621459.1968.10480934.

Sitayeb, T. & Benabdeli, K. 2008 Contribution à l'étude de la dynamique de l'occupation des sols de la plaine de la Macta (Algérie) à l'aide de la télédétection et des systèmes d'information géographique. *C. R. Biol.* **331**, 466–474. doi:10.1016/j.crvi.2008.03.010.

Souidi, Z., Miara, M., Benhanifia, K., Daikh, A. & Moumenine, A. 2016 *Guide de terrain des plantes spontanées de la zone humide des marais de la Macta.* INAS Edition, Alger, Algérie.

Stellmes, M., Udelhoven, T., Röder, A., Sonnenschein, R. & Hill, J. 2010 Dryland observation at local and regional scale: comparison of Landsat TM/ETM+ and NOAA AVHRR time series. *Remote Sens. Environ.* **114** (10), 2111–2125. doi:10.1016/j.rse.2010.04.016.

Suryavanshi, S., Pandey, A., Chaube, U. C. & Joshi, N. 2014 Long-term historic changes in climatic variables of Betwa Basin, India. *Theor. Appl. Climatol.* **117**, 403–418. doi:10.1007/s00704-013-1013-y.

Tabari, H., Somee, B. S. & Zadeh, M. R. 2011 Testing for long-term trends in climatic variables in Iran. *Atmos. Res.* **100**, 132–140. doi:10.1016/j.atmosres.2011.01.005.

Tucker, C. J., Fung, I. Y., Keeling, C. D. & Gammon, R. H. 1986 Relationship between atmospheric CO_2 variations and a satellite-derived vegetation index. *Nature* **319**, 195–199. doi:10.1038/319195a0.

Wang, Y. T., Xie, D. H. & Li, Y. H. 2014 Downscaling remotely sensed land surface temperature over urban areas using trend surface of spectral index. *J. Remote Sens.* **18**, 1169–1181. doi:10.11834/jrs.20144115.

Wang, C., Chen, J., Tang, Y., Black, T. A. & Zhu, K. 2018 A novel method for removing snow melting-induced fluctuation in GIMMS NDVI3g data for vegetation phenology monitoring: a case study in deciduous forests of North America. *IEEE J. Sel. Topics Appl. Earth Observ. Remote Sens.* **11** (3), 800–807. doi:10.1109/JSTARS.2017.2778076.

Wu, D., Zhao, X., Liang, S., Zhou, T., Huang, K., Tang, B. & Zhao, W. 2015 Time-lag effects of global vegetation responses to climate change. *Glob. Change Biol.* **21**, 3520–3531. doi:10.1111/gcb.12945.

Xie, F. & Fan, H. 2021 Deriving drought indices from MODIS vegetation indices (NDVI/EVI) and Land Surface Temperature (LST): is data reconstruction necessary? *Int. J. Appl. Earth Observation Geoinformation* **101**, 102352. doi:10.1016/j.jag.2021.102352.

Xu, N., Deng, F., Liu, B. Q., Li, C. X., Fu, H. C., Yang, H. & Zhang, J. H. 2021 Changes in the urban surface thermal environment of a Chinese coastal city revealed by downscaling MODIS LST with random forest algorithm. *J. Meteor. Res.* **35** (5), 759–774. doi:10.1007/s13351-021-0023-4.

Xue, J. & Su, B. 2017 Significant remote sensing vegetation indices: a review of developments and applications. *J. Sens.* **2017**, 1353691. doi:10.1155/2017/1353691.

Yang, J., Sun, J., Ge, Q. S. & Li, X. M. 2017 Assessing the impacts of urbanization-associated green space on urban land surface temperature: a case study of Dalian, China. *Urban Forestry Urban Green.* **22**, 1–10. doi:10.1016/j.ufug.2017.01.002.

Zhe, M. & Zhang, X. 2021 Time-lag effects of NDVI responses to climate change in the Yamzhog Yumco Basin, South Tibet. *Ecol. Indic.* **124**, 107431. doi:10.1016/j.ecolind.2021.107431.

Zhu, Z., Piao, S., Myneni, R. B., Huang, M., Zeng, Z., Canadell, J. G., Ciais, P., Sitch, S., Friedlingstein, P., Arneth, A., Cao, C., Cheng, L., Kato, E., Koven, C., Li, Y., Lian, X., Liu, Y., Liu, R., Mao, J., Pan, Y., Peng, S., Peñuelas, J., Poulter, B., Pugh, T. A. M., Stocker, B. D., Viovy, N., Wang, X., Wang, Y., Xiao, Z., Yang, H., Zaehle, S. & Zeng, N. 2016 Greening of the Earth and its drivers. *Nat. Clim. Change* **6**, 791. doi:10.1038/nclimate3004.

First received 25 July 2023; accepted in revised form 6 March 2024. Available online 19 March 2024